J|A|C|S
ARTICLES
Published on Web 06/05/2007

Prototypical Phosphorus Analogues of Ethane: General and Versatile Synthetic Approaches to Hexaalkylated P−P Diphosphonium Cations

Jan. J. Weigand,[†] Susanne D. Riegel,[†] Neil Burford,*[,†] and Andreas Decken[‡]

Contribution from the Department of Chemistry, Dalhousie University, Halifax, NS, B3H 4J3, Canada, and the Department of Chemistry, University of New Brunswick, Fredericton, NB, E3A 6E2, Canada

Received February 28, 2007; E-mail: neil.burford@dal.ca

Abstract: Versatile alkylation reactions give access to symmetric, homoleptic nonsymmetric, and heteroleptic symmetric hexaalkylated 1,2-diphosphonium derivatives as bottleable salts in high yields. A series of 1,2-diphosphonium salts has been isolated and characterized, representing prototypical phosphorus analogues of ethane. Additionally, the solid-state structures for four derivatives have been determined crystallographically. Nonsymmetrically substituted derivatives of 1,2-diphosphonium cations enable the direct observation of $^1J(P_AP_B)$ coupling constants for two tetracoordinate phosphorus centers. The synthetic approaches promise access to a vast array of derivatives and will provide means to the systematic development of phosphorus analogues of hydrocarbon chemistry.

Introduction

The C−C homoatomic bond is fundamentally responsible for the extent and diversity of organic chemistry. Homoatomic bonding is prevalent for other nonmetal elements but is most developed for phosphorus, consistent with the diagonal relationship between carbon and phosphorus.[1] Series of *catena*-phosphines,[2−5] *catena*-phosphinophosphide anions,[2−4,6] and *catena*-phosphinophosphonium cations[7−13] have been reported, but many of the frameworks observed in carbon chemistry have not been replicated in the chemistry of phosphorus.

The fundamentally important parent or benchmark P−P bonded diphosphonium unit is present in a few structurally characterized compounds that involve sterically bulky amine substituents (**1**[14]) or a polycyclic framework (**2**,[15] **3**,[16] and **4**[17]). Nevertheless, hexaalkyldiphosphonium triiodide salts are speculated as the products of reactions of red phosphorus with alkyl iodides or from trialkylphosphines with iodine,[18,19] and $[Me_3PPMe_3][PF_6]_2$ has been assigned on the basis of elemental analysis data and IR spectroscopy.[20] We have now discovered that alkylation reactions of diphosphines or phosphinophosphonium cations provide a versatile approach to hexaalkyl-1,2-diphosphonium dications, representing prototypical phosphorus analogues of ethane. Six derivatives have been characterized as either trifluoromethanesulfonate (OTf) or tetrachlorogallate

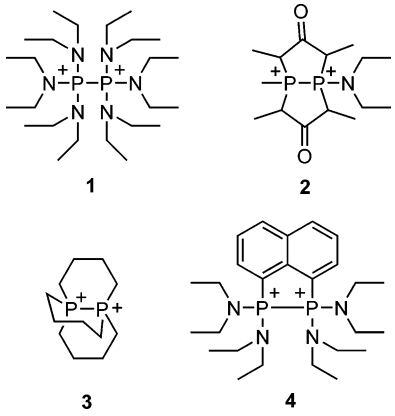

[†] Dalhousie University.
[‡] University of New Brunswick.

(1) Dillon, K. B.; Mathey, F.; Nixon, J. F. *Phosphorus: The Carbon Copy*; John Wiley & Sons: 1997.
(2) Baudler, M. *Angew. Chem., Int. Ed. Engl.* **1982**, *21*, 492−512.
(3) Baudler, M. *Angew. Chem., Int. Ed. Engl.* **1987**, *26*, 419−441.
(4) Baudler, M.; Glinka, K. *Chem. Rev.* **1993**, *93*, 1623−1667.
(5) Baudler, M.; Glinka, K. *Chem. Rev.* **1994**, *94*, 1273−1297.
(6) Geier, J.; Harmer, J.; Grutzmacher, H. *Angew. Chem., Int. Ed.* **2004**, *43*, 4093−4097.
(7) Burford, N.; Ragogna, P. J.; McDonald, R.; Ferguson, M. *J. Am. Chem. Soc.* **2003**, *125*, 14404−14410.
(8) Burford, N.; Ragogna, P. J. *Dalton Trans.* **2002**, 4307−4315.
(9) Burford, N.; Herbert, D. E.; Ragogna, P. J.; McDonald, R.; Ferguson, M. J. *J. Am. Chem. Soc.* **2004**, *126*, 17067−17073.
(10) Burford, N.; Dyker, C. A.; Decken, A. *Angew. Chem., Int. Ed.* **2005**, *44*, 2364−2367.
(11) Burford, N.; Dyker, C. A.; Lumsden, M. D.; Decken, A. *Angew. Chem., Int. Ed.* **2005**, *44*, 6196−6199.
(12) Weigand, J. J.; Burford, N.; Lumsden, M. D.; Decken, A. *Angew. Chem., Int. Ed.* **2006**, *45*, 6733−6737.
(13) Dyker, C. A.; Burford, N.; Lumsden, M. D.; Decken, A. *J. Am. Chem. Soc.* **2006**, *128*, 9632−9633.
(14) Nikitin, E. V.; Romakhin, A. S.; Zagumennov, V. A.; Babkin, Yu, A. *Electrochim. Acta* **1997**, *42*, 2217−2224.
(15) Schomburg, D.; Bettermann, G.; Ernst, L.; Schmutzler, R. *Angew. Chem., Int. Ed. Engl.* **1985**, *24*, 975−976.
(16) Alder, R. W.; Ganter, C.; Harris, C. J.; Orpen, A. G. *Chem. Commun.* **1992**, 1172−1174.
(17) Kilian, P.; Slawin, A. M. Z.; Woollins, J. D. *Dalton Trans.* **2006**, 2175−2183.
(18) Makovetskii, Y. P.; Feshchenko, N. G.; Malovik, V. V.; Semenii, V. Y.; Boldeskul, I. E.; Bondar, V. A.; Chernukho, N. P. *Zh. Obshch. Khim.* **1980**, *50*, 1967.
(19) Makovetskii, Y. P.; Lidkovskii, V. E.; Boldeskul, I. E.; Feshchenko, N. G.; Kalibabchuk, N. N. *Zh. Obshch. Khim.* **1989**, *52*, 1989.
(20) Siddique, R. M.; Winfield, J. M. *Can. J. Chem.* **1989**, *67*, 1780−1784.

($GaCl_4$) salts. These new dications provide a foundational origin for the fundamental chemistry of phosphorus.

Experimental Section

Caution: Many phosphines are pyrophoric and very toxic compounds. Methyl triflate (MeOTf) is a highly volatile, powerful methylating agent that reacts violently. All manipulations should be carried out under inert N_2 atmosphere and on a small scale (0.5 to 1.0 mmol).

General Remarks. All reactions were carried out in a glovebox under an inert N_2 atmosphere. Solvents were dried on an MBraun solvent purification system and stored under nitrogen and over molecular sieves prior to use. Anhydrous MeCN was purchased from Sigma-Aldrich and used as received. Me_2PPMe_2 was prepared according to the literature method.[21] ^{t}BuCl and Me_3SiOTf were purchased from Sigma-Aldrich, Me_2PCl was purchased from Strem, and all were vacuum distilled prior to use. PMe_3 in toluene, PEt_3, P^nPr_3, P^iPr_3, $^tBu_2PCl$, MeOTf, and $GaCl_3$ were purchased from Sigma-Aldrich and used as received. NMR: Bruker AVANCE 500 (^{1}H (500.13 MHz), ^{13}C (125.76 MHz) chemical shift referenced to $\delta_{TMS} = 0.00$; ^{31}P (202.46 MHz) to $\delta_{H3PO4(85\%)} = 0.00$) and are reported in ppm; J values are reported in Hz. Bruker AC-250 (^{19}F (235.35 MHz) chemical shifts are reported in ppm and referenced to $\delta_{C6H5CF3} = -63.72$. ^{31}P NMR parameters were derived by fitting the observed experimental spectra with a computer simulation using the software program gNMR, version 5.0, by Cherwell Scientific.[22] Melting points were recorded on an Electrothermal melting point apparatus in sealed capillary tubes under N_2 and are uncorrected. Raman spectra were obtained for powdered and crystalline samples on a Bruker RFS 100 instrument equipped with an Nd:YAG laser (1064 nm). Chemical analyses were determined by Canadian Microanalytical Service Ltd., Delta, BC, Canada.

General Procedure for the Preparation of Phosphinophosphonium Salts [$R_3P-PR'_2$][OTf] (6a−e[OTf]): Me_3SiOTf (180 μL, 1.00 mmol) was added dropwise to a mixture of the trialkylphosphine (1.00 mmol) and the corresponding dialkylchlorophosphine (1.00 mmol) in CH_2Cl_2 (10 mL). The solution was stirred for 30 min and concentrated *in vacuo* to 5 mL. Addition of Et_2O (∼15 mL) afforded the crude phosphinophosphonium salt as a white precipitate. After isolation and washing (Et_2O, 3 × 5 mL), pure compounds were obtained by vapor diffusion of Et_2O into a CH_3CN solution of the corresponding salt.

[Me_3P-PMe_2][OTf] (6a[OTf]): 270 mg (94%); mp 222−226 °C; Raman (250 mW, 25 °C, cm^{-1}): 2992 (48), 2918 (100), 1495 (7), 1414 (9), 1226 (6), 1035 (36), 757 (15), 713 (7), 682 (23), 574 (6), 445 (15), 349 (10), 314 (11), 238 (12), 84 (54); ^{31}P{^{1}H} NMR (d_3-MeCN, 300 K, [ppm]): $\delta_a = 17.60$ (*d*); $\delta_b = -59.35$ (*d*), $^1J_{PP} = -274.3$ Hz.

[Et_3P-PMe_2][OTf] (6b[OTf]): 293 mg (89%); mp 208−211 °C; Raman (250 mW, 25 °C, cm^{-1}): 2989 (58), 2950 (74), 2917 (100), 2888 (30), 1412 (12), 1266 (7), 1224 (94), 1032 (53), 754 (19), 712 (13), 665 (16), 620 (14), 572 (10), 500 (12), 348 (17), 337 (18), 313 (15), 231 (13), 120 (13), 85 (94); ^{31}P{^{1}H} NMR (d_3-MeCN, 300 K, [ppm]): $\delta_a = 32.28$ (*d*); $\delta_b = -63.08$ (*d*), $^1J_{PP} = -294.3$ Hz.

[$^nPr_3P-PMe_2$][OTf] (6c[OTf]): 296 mg (80%); mp 54−59 °C; Raman (250 mW, 25 °C, cm^{-1}): 2979 (53), 2938 (88), 2916 (100), 2878 (59), 2738 (8), 1495 (11), 1452 (15), 1412 (11), 1312 (8), 1224 (10), 1085 (7), 1030 (59), 753 (19), 713 (10), 667 (15), 572 (9), 347 (16), 312 (23), 235 (11), 117 (15); ^{31}P{^{1}H} NMR (d_3-MeCN, 300 K, [ppm]): $\delta_a = 24.20$ (*d*); $\delta_b = -60.22$ (*d*), $^1J_{PP} = -296.0$ Hz.

[$^iPr_3P-PMe_2$][OTf] (6d[OTf]): 191 mg (98%); mp 51−56 °C; Raman (250 mW, 25 °C, cm^{-1}): 2979 (72), 2916 (100), 2738 (6), 1495 (11), 1477 (13), 1260 (6), 1225 (8), 1067 (6), 1031 (41), 883 (13), 752 (18), 715 (9), 673 (14), 573 (8), 446 (14), 347 (13), 312 (26), 180 (13), 119 (19); ^{31}P{^{1}H} NMR (d_3-MeCN, 300 K, [ppm]): $\delta_a = 36.38$ (*d*); $\delta_b = -54.77$ (*d*), $^1J_{PP} = -331.9$ Hz.

[$Me_3P-P^tBu_2$][OTf] (6e[OTf]): 283 mg (76%); mp 129−134 °C; Raman (250 mW, 25 °C, cm^{-1}): 2995 (40), 2969 (41), 2924 (100), 2907 (62), 2877 (26), 2870 (21), 1474 (12), 1449 (12), 1032 (36), 804 (15), 754 (18), 679 (18), 567 (16), 348 (11), 314 (12), 271 (18), 121 (10), 84 (86), 71 (10); ^{31}P{^{1}H} NMR (d_3-MeCN, 300 K, [ppm]): $\delta_a = 42.26$ (*d*); $\delta_b = 10.81$ (*d*), $^1J_{PP} = -382.6$ Hz.

General Procedure for the Preparation and Isolation of 7[OTf]$_2$ from 6[OTf]: Excess MeOTf (181 μL, 2.5 mmol, 5 equiv) was added to the corresponding phosphinophosphonium salt (0.5 mmol) and the mixture was stirred, yielding a viscous colorless oil that solidified after approximately 1 to 3 min. The crude material was recrystallized from a mixture of MeCN/MeOTf (3 mL/100 μL) that was layered with Et_2O (5 mL) and stored in the freezer (−32 °C) for 12 to 24 h. Crystals suitable for X-ray diffraction were obtained by dissolving the sample (0.050−0.100 g) in minimal MeCN/MeOTf in an uncapped 1 dram vial, which was placed inside a 4 dram vial containing Et_2O. The larger vial was capped, and the system was allowed to stand in a freezer until crystals of suitable quality formed. In solution, all derivatives of **7**[OTf]$_2$ are highly moisture sensitive and very reactive and decompose within a few hours; recrystallization must be performed quickly. Samples prepared to obtain NMR spectra contained excess MeOTf (10%).

[Me_3P-PMe_3][OTf]$_2$ (7a[OTf]$_2$) from Tetramethyldiphosphine: Excess MeOTf (565 μL, 5 mmol) was added to neat tetramethyldiphosphine (122 mg, 1.0 mmol) leading to the instantaneous and exergonic formation of a white solid.

[Me_3P-PMe_3][OTf]$_2$ (7a[OTf]$_2$): 424 mg (94%); mp 217−219 °C; Raman (250 mW, 25 °C, cm^{-1}): 3008 (29), 2986 (41), 2919 (100), 1495 (18), 1400 (20), 1257 (20), 1229 (18), 1030 (43), 782 (15), 759 (24), 689 (19), 575 (20), 455 (17), 348 (19), 320 (19), 297 (17), 237 (21), 118 (10); ^{1}H NMR (d_3-MeCN, 300 K, [ppm]): $\delta = 2.39$ (18 H, *m, A part of an $A_9A_9'M_3M_3'XX'$ system*, $^2JH_AP_X = {}^2JH_{A'}P_{X'} = -14.6$ Hz, $^3JH_AP_{X'} = {}^3JH_{A'}P_X = 8.6$ Hz); ^{13}C NMR (d_3-$MeNO_2$, 300 K, [ppm]): $\delta = 7.1$ (6 Me, *m, M part of an $A_9A_9'M_3M_3'XX'$ system*, $^1JC_MP_X = {}^1JH_{M'}P_{X'} = -2.7$ Hz, $^2JH_MP_{X'} = {}^2JH_{M'}P_X = -43.0$ Hz); ^{31}P NMR (d_3-$MeNO_2$, 300 K, [ppm]): $\delta = 28.44$ (2 P, *m, X part of an $A_9A_9'M_3M_3'XX'$ system*, $^1JP_XP_{X'} = -19.9$ Hz); ^{19}F NMR (d_3-MeCN, 300 K, [ppm]): $\delta = -79.4$ ($-CF_3$, *s*). Elemental analysis for $C_8H_{18}F_6O_6P_2S_2$ (450.29) calcd: C, 21.34; H, 4.03. Found: C, 22.69; H, 4.09. Compound decomposes under vacuum.

[Et_3P-PMe_3][OTf]$_2$ (7b[OTf]$_2$): 450 mg (92%); mp 67−69 °C; Raman (250 mW, 25 °C, cm^{-1}): 2992 (45), 2960 (56), 2919 (100), 2415 (19), 1411 (15), 1359 (10), 1226 (18), 1032 (88), 774 (10), 758 (33), 672 (20), 575 (23), 519 (9), 469 (11), 404 (10), 350 (35), 315 (26), 252 (16), 123 (14), 84 (43); ^{1}H{^{31}P} NMR (d_3-MeCN, 300 K, [ppm]): $\delta = 1.58$ (9H, *t*, $CH_2\boldsymbol{Me}$, $^3J_{HH} = 7.5$ Hz), 2.62 (9H, *s*, ***Me***); 3.02 (6H, *q*, $C\boldsymbol{H}_2Me$, $^3J_{HH} = 7.8$ Hz), ^{13}C NMR (d_3-MeCN/MeOTf (stabilized), [ppm]): 6.0 (3C, *dd*, $CH_2\mathbf{Me}$, $^2JC_{CH_2\boldsymbol{Me}}P_\alpha = -2.9$ Hz, $^3JC_{CH_2\boldsymbol{Me}}P_\beta = 6.2$ Hz), $\delta = 7.6$ (3C, *d(broad)*, ***Me***, $^1JC_{\boldsymbol{Me}}P_\beta = 42.4$ Hz), 11.8 (3C, *d(broad)*, $\boldsymbol{C}H_2Me$, $^2JC_{\boldsymbol{C}H_2Me}P_\beta = 33.8$ Hz); ^{31}P NMR (d_3-MeCN, 300 K, [ppm]): $\delta = 28.22$ (P_β, *d*), 37.12 (P_α, *d*), $^1JP_\alpha P_\beta = -48.9$ Hz; ^{19}F NMR (d_3-MeCN, 300 K, [ppm]): $\delta = -79.4$ ($-CF_3$, *s*).

[$^nPr_3P-PMe_3$][OTf]$_2$ (7c[OTf]$_2$): 0.289 mg (99%); mp 201−203 °C; Raman (250 mW, 25 °C, cm^{-1}): 3007 (29), 2986 (41), 2918 (100), 1495 (18), 1399 (20), 1256 (20), 1228 (18), 1029 (43), 781 (15), 758 (24), 688 (19), 574 (20), 454 (17), 348 (18), 319 (19), 296 (17), 237 (21), 117 (10); ^{1}H{^{31}P} NMR (d_3-MeCN, 300 K, [ppm]): $\delta = 1.17$ (9H, *t*, $CH_2CH_2\boldsymbol{Me}$), 1.80 (6H, *m*, $CH_2C\boldsymbol{H}_2Me$), 2.45 (9H, *s*, ***Me***), 2.76 (6H, *m*, $C\boldsymbol{H}_2CH_2Me$); ^{13}C NMR (d_3-MeCN/MeOTf (stabilized), [ppm]): $\delta = 7.3$ (3C, *dd*, ***Me***, $^1JC_{\boldsymbol{Me}}P_\beta = 1.7$ Hz, $^2JC_{\boldsymbol{Me}}P_\alpha = 41.8$ Hz), 14.5 (3C, *d*, $CH_2CH_2\boldsymbol{Me}$, $^3JC_{CH_2CH_2\boldsymbol{Me}}P_\alpha = -19.2$ Hz, $^4JC_{CH_2CH_2\boldsymbol{Me}}P_\beta = 0.8$), 16.3 (3C, *dd*, $CH_2\boldsymbol{C}H_2Me$, $^2JC_{CH_2\boldsymbol{C}H_2Me}P_\alpha = 5.2$ Hz, $^3JC_{CH_2\boldsymbol{C}H_2Me}P_\beta = -2.8$ Hz), 19.4 (3C, *dd*, $\boldsymbol{C}H_2CH_2Me$, $^1JC_{CH_2\boldsymbol{C}H_2Me}P_\alpha = 1.8$ Hz, $^2JC_{\boldsymbol{C}H_2CH_2Me}P_\beta = 31.4$ Hz); ^{31}P NMR (d_3-MeCN, 300 K, [ppm]): $\delta =$

(21) Butter, S. A.; Chatt, J. *Inorg. Synth.* **1974**, *15*, 185−191.
(22) Budzelaar, P. H. M. *gNMR for Windows* (4.0) The Magdalen Centre, Oxford Science Park, Oxford OX4 4GA, UK, Cherwell Scientific Publishing Limited: 1997.

28.08 (P_β, *d*), 29.30 (P_α, *d*), $^1JP_\alpha P_\beta = -48.1$ Hz; ^{19}F NMR (d_3-MeCN, 300 K, [ppm]): $\delta = -79.5$ ($-CF_3$, s). Elemental analysis for $C_{14}H_{30}F_6O_6P_2S_2$ (534.45) calcd: C, 31.46; H, 5.66. Found: C, 31.47; H, 5.72.

[^{i}Pr$_3$P−PMe$_3$][OTf]$_2$ (7d[OTf]$_2$): *The preparation differs from the general procedure:* Excess MeOTf (2.5 mL, 20 mmol, 20 equiv) was added under stirring to the corresponding phosphinophosphonium salt (1 mmol) at once. The obtained suspension was stirred for 6 h. The addition of acetonitrile (3 mL) yielded a clear solution from which layering with Et_2O yielded irregular rods of **7d** after 12 h (−32 °C): 491 mg (92%); mp 166−167 (sharp) °C; Raman (250 mW, 25 °C, cm^{-1}): 2987 (52), 2953 (52), 2930 (47), 2910 (100), 1494 (20), 1472 (21), 1396 (18), 1256 (17), 1227 (20), 1088 (16), 1031 (86), 869 (18), 780 (17), 758 (39), 679 (26), 574 (28), 503 (26), 417 (20), 349 (40), 314 (32), 217 (28), 186 (24), 121 (20); ^{1}H NMR (d_3-MeCN/MeOTf (stabilized), 300 K, [ppm]): $\delta = 1.62$ (18H, *dd*, CH***Me***$_2$, $^2JH_{CHMe_2}H_{CHMe_2} = 7.2$ Hz, $^3JH_{CHMe_2}P_\alpha = 0.5$, $^4JH_{CHMe_2}P_\beta = 18.7$ Hz), 2.54 (9H, *dd*, ***Me***, $^2JH_{Me}P_\alpha = 6.2$, $^3JH_{Me}P_\beta = -13.6$ Hz), 3.46 (3H, *m*, C***H***Me$_2$, $^2JH_{CHMe_2}P_\alpha = 6.7$, $^3JH_{CHMe_2}P_\beta = -10.9$ Hz); ^{13}C NMR (d_3-MeCN/MeOTf (stabilized), [ppm]): $\delta = 10.4$ (3C, *d(broad)*, ***Me***, $^1JC_{Me}P_\beta = 40.9$ Hz), 17.1 (3C, *dd*, CH***Me***$_2$, $^2JC_{Me}P_\beta = 3.3$ Hz, $^3JC_{Me}P_\alpha = -2.4$), 23.7 (3C, *dd*, ***C***H**Me**$_2$, $^1JC_{CHMe_2}P_\alpha = 22.9$ Hz, $^2JC_{CHMe_2}P_\beta = -1.9$ Hz); ^{31}P NMR (d_3-MeCN, 300 K, [ppm]): $\delta = 28.86$ (P_β, *d*), 46.91 (P_α, *d*), $^1JP_\alpha P_\beta = -74.4$ Hz; ^{19}F NMR (d_3-MeCN, 300 K, [ppm]): $\delta = -79.5$ ($-CF_3$, *s*). Elemental analysis for $C_{14}H_{30}F_6O_6P_2S_2$ (534.45) calcd: C, 31.46; H, 5.66. Found: C, 31.77; H, 5.29.

[Me$_3$P−P^{t}Bu$_2$Me][OTf]$_2$ (7e[OTf]$_2$): 230 mg (86%); mp 97−100 °C; Raman (250 mW, 25 °C, cm^{-1}): 3010 (30), 2980 (59), 2946 (45), 2917 (100), 1495 (7), 1472 (13), 1417 (9), 1226 (10), 1173 (8), 1036 (76), 932 (5), 800 (13), 760 (32), 677 (19), 574 (18), 518 (5), 498 (10), 351 (21), 318 (19), 270 (18). 242 (16), 155 (11), 118 (10); ^{1}H NMR (d_3-MeCN, 300 K, [ppm]): $\delta = 1.67$ (18H, *d*, C***Me***$_3$, $^3JH_{CMe_3}P_\alpha = 18.7$), 2.44 (3H, *dd*, ***Me***, $^2JH_{Me}P_\alpha = 11.5$, $^3JH_{Me}P_\beta = -10.1$ Hz), 2.60 (9H, *dd*, ***Me***, $^2JH_{Me}P_\beta = 6.1$, $^3JH_{Me}P_\alpha = 13.4$ Hz); ^{13}C NMR (d_3-MeCN, 300 K, [ppm]): $\delta = 9.3$ (1C, *dd*, ***Me***, $^1JC_{Me}P_\alpha = 7.3$ Hz, $^2JC_{Me}P_\beta = 42.8$ Hz), 11.6 (3C, *d*, ***Me***, $^1JC_{Me}P_\beta = 1.0$ Hz, $^2JC_{Me}P_\alpha = -40.5$ Hz), 28.1 (6C, *dd*, C***Me***$_3$, $^2JC_{CMe_3}P_\alpha = 6.2$ Hz, $^3JC_{CMe_3}P_\beta = -14.2$ Hz), 41.1 (2C, *d*, ***C***Me$_3$, $^1JC_{CMe_3}P_\alpha = 1.1$ Hz, $^2JC_{CMe_3}P_\beta = 16.7$ Hz); ^{31}P NMR (d_3-MeCN, 300 K, [ppm]): $\delta = 32.23$ (P_β, *d*), 54.58 (P_α, *d*), $^1JP_\alpha P_\beta = -93.6$ Hz; ^{19}F NMR (d_3-MeCN, 300 K, [ppm]): $\delta = -79.5$ ($-CF_3$, *s*). Elemental analysis for $C_{14}H_{30}F_6O_6P_2S_2$ (534.45) calcd: C, 31.46; H, 5.66. Found: C, 31.83; H, 5.70.

[^{t}BuMe$_2$P−PMe$_2$^{t}Bu][GaCl$_4$]$_2$ (7i[GaCl$_4$]$_2$): Solid $GaCl_3$ (120 mg, 0.69 mmol) was added to a stirred solution of Me_2PPMe_2 (40 mg, 0.34 mmol) in benzene (4 mL) yielding a white precipitate that is tentatively assigned as the adduct $GaCl_3Me_2PPMe_2GaCl_3$. The dropwise addition of ^{t}BuCl (74.9 μL, 0.69 mmol) leads to the dissolution of the precipitate and reprecipitation of a new white solid. After 40 min Et_2O (10 mL) was added, and the resultant white precipitate was isolated and washed with Et_2O (3 × 3 mL). The crystalline product was obtained from the room-temperature diffusion of Et_2O vapor into a MeCN solution of the white precipitate; 170 mg (85%); mp 158−162 °C; Raman (250 mW, 25 °C, cm^{-1}): 2984 (45), 2974 (66), 2947 (37), 2920 (100), 2908 (72), 1461 (11), 1443 (8), 1396 (11), 1379 (6), 1198 (6), 1020 (5), 799 (9), 770 (7), 721 (10), 663 (5), 591 (16), 476 (15), 383 (12), 345 (66), 228 (20), 153 (36), 121 (36); ^{1}H{^{31}P} NMR (d_3-MeCN, 300 K, [ppm]): $\delta = 1.58$ (18H, *s*, C***Me***$_3$), 2.40 (12H, *s*, ***Me***); ^{13}C NMR (d_3-MeCN, 300 K, [ppm]): $\delta = 5.0$ (4C, *t*, ***Me***, $^1JC_{Me}P_\alpha = 18.9$ Hz, $^2JC_{Me}P_\beta = 20.2$ Hz), 25.1 (6C, *s*, C***Me***$_3$, not resolved, $^2JC_{CMe_3}P_\alpha = -1.7$ Hz, $^3JC_{CMe_3}P_\beta = 1.2$), 38.2 (2C, *t*, ***C***Me$_3$, $^1JC_{CMe_3}P_\alpha = 11.7$ Hz, $^2JC_{CMe_3}P_\beta = -12.6$ Hz); ^{31}P NMR (d_3-MeCN, 300 K, [ppm]): $\delta = 45.8$ (2P, *s*, $^1JP_\alpha P_\beta = -94.2$ Hz). Elemental analysis for $C_{12}H_{30}Cl_8Ga_2P_2$ (659.38) calcd: C, 21.86; H, 4.59. Found: C, 22.30; H, 4.80.

Crystallography. Single crystals of **7a**[OTf]$_2$, **7b**[OTf]$_2$, **7d**[OTf]$_2$, and **7i**[$GaCl_4$]$_2$ were coated with Paratone-N oil, mounted using a 20 micron cryo-loop, and frozen in the cold nitrogen stream of the goniometer. A hemisphere of data was collected on a Bruker AXS P4/SMART 1000 diffractometer using ω and θ scans with a scan width of 0.3° and 10 s (**7a**[OTf]$_2$, **7b**[OTf]$_2$), 20 s (**7d**[OTf]$_2$), and 30 s (**7i**[$GaCl_4$]$_2$) exposure times. The detector distance was 5 cm in all cases. For **7a**[OTf]$_2$, **7b**[OTf]$_2$, and **7i**[$GaCl_4$]$_2$, the data were reduced (SAINT 6.02, 1997−1999, Bruker AXS, Inc., Madison, Wisconsin) and corrected for absorption (SADABS George Sheldrick, 1999, Bruker AXS, Inc., Madison, Wisconsin). In the case of **7d**[OTf]$_2$, the crystal was twinned and the orientation matrixes for the major component were determined (CELL_NOW, 2005 George Sheldrick, Bruker AXS, Inc., Madison, Wisconsin). The data were reduced (SAINT) and corrected for absorption (TWINABS 1.05, George Sheldrick, 2004, Bruker Nonius, Inc., Madison, Wisconsin). The angle between the two components of the twinned crystal was so small that twin refinement resulted in high esd's for bond length and angles. Refinement using a single crystal approach resulted in a 94% data completeness to 55° in 2θ. The structures were solved by direct methods and refined by full-matrix least-squares on F^2 (SHELXTL 6.14, 2000−2003, Bruker AXS, Inc., Madison, Wisconsin). In the case of **7b**[OTf]$_2$, one of the PEt_3 groups is disordered and the site occupancy was determined using an isotropic model as 0.6 (P(3), C(11)−C(15)) and 0.4 (P(3′), C(11″)−C(15′)) and was fixed in subsequent refinement cycles. All non-hydrogen atoms were refined anisotropically. For **7b**[OTf]$_2$ and **7i**[$GaCl_4$]$_2$ hydrogen atoms were included in calculated positions and refined using a riding model. In the case of **7a**[OTf]$_2$ and **7d**[OTf]$_2$, hydrogen atoms were found in Fourier difference maps and refined isotropically.

Results and Discussion

Synthesis and Characterization. Chlorophosphinophosphonium **5** salts are generally prepared via chloride ion abstraction from a chlorophosphine according to Scheme 1a or b.[7,23] While the reaction can be considered as the formation of a coordinate P−P bond between a phosphine and a phosphenium cation,[8] the phosphinophosphonium bonding model **5**[8] defines the framework as a chlorophosphonio-phosphine derived from a diphosphine. As illustrated in Scheme 1c, in the presence of a trialkyl- or triaryl-phosphine, chloride ion abstraction from a chlorophosphine affords a phosphinophosphonium cation **6**, for which heteroleptic derivatives (**6f** and **6g**)[7] and homoleptic derivatives (**6a**[10] and **6h**[7]) have been reported. We have employed this versatile approach (Scheme 1c) to extend the series of fundamental and prototypical phosphinophosphonium cations to include the heteroleptic derivatives **6b**, **6c**, **6d**, and **6e**.

As each derivative of **6** can be envisaged as an alkylation product of a diphosphine (R_2PPR_2), we have investigated the reactions of diphosphines with alkylating agents, as previously reported for the diphosphene, Mes*P═PMes*, which gives the methylated phosphanyl-phosphenium triflate [Mes*(Me)P═PMes*][OTf].[24] Similarly, ^{31}P{^{1}H} NMR spectra of reaction mixtures containing Me_4P_2 and MeOTf in CH_2Cl_2 show two doublets that are characteristic of [Me_5P_2][OTf], **6a**[OTf],[10] as depicted in Scheme 2a. While the preparation of [Mes*(Me)P═PMes*][OTf] requires a vast excess of MeOTf (35-fold),[24] **6a**[OTf] is formed as the sole product in an equimolar reaction mixture of Me_4P_2 and MeOTf in CH_2Cl_2 (Scheme 2a), independent of stoichiometry.

Conversely, the reaction of Me_4P_2 in neat MeOTf occurs as a slurry which dissolves in nitromethane and shows (^{31}P{^{1}H}

(23) Burford, N.; Cameron, T. S.; LeBlanc, D. J.; Losier, P.; Sereda, S.; Wu, G. *Organometallics* **1997**, *16*, 4712−4717.
(24) Loss, S.; Widauer, C.; Grützmacher, H. *Angew. Chem., Int. Ed.* **1999**, *38*, 3329−3331.

Scheme 1

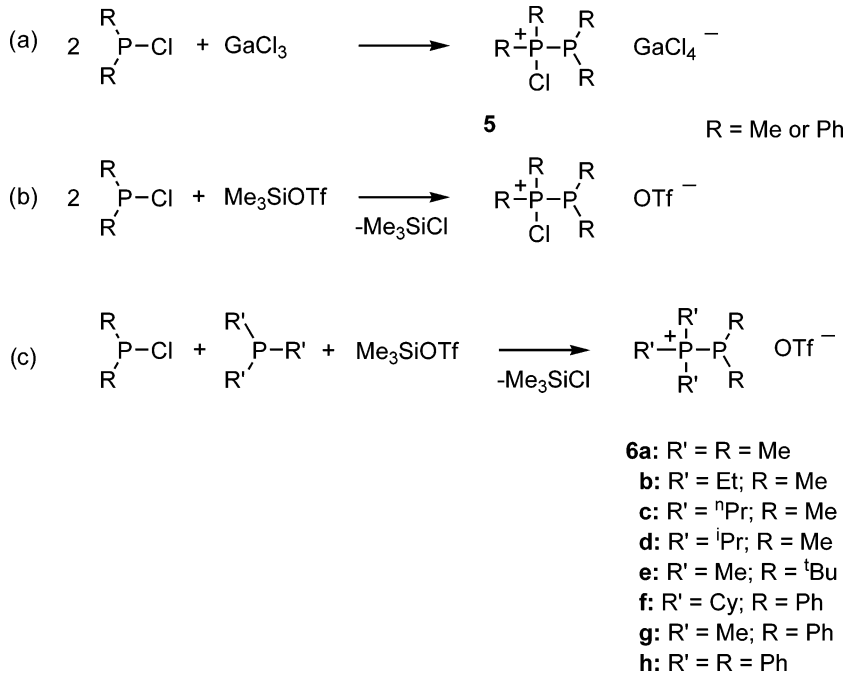

Scheme 2

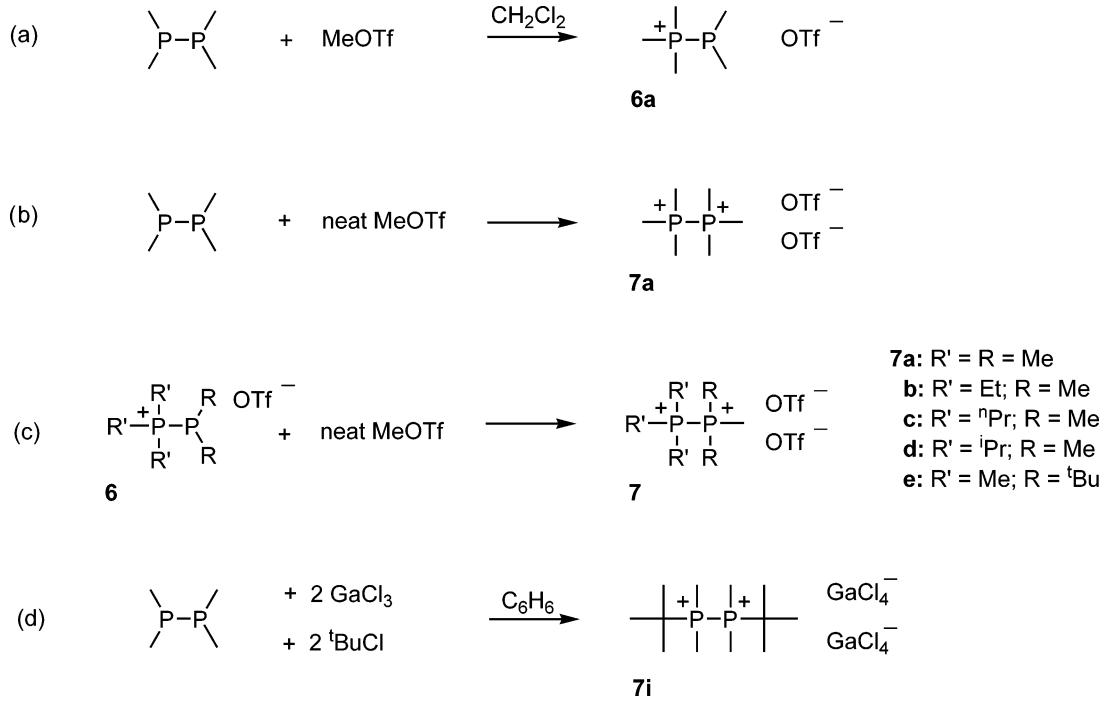

NMR spectrum of the reaction mixture) quantitative conversion to the symmetric dialkylated product $[Me_6P_2][OTf]_2$, **7a**$[OTf]_2$ (Scheme 2b). As illustrated in Scheme 2c, **7a**$[OTf]_2$ is also observed ($^{31}P\{^1H\}$ NMR spectra) as the only product in reaction mixtures of **6a**[OTf] and neat MeOTf. Therefore, alkylation of Me_4P_2, or derivatives of **6**, offers a versatile synthetic approach to access a potentially vast array of hexaalkylated 1,2-diphosphonium dications. This is demonstrated by the high yield preparation (>90%) of compounds **7b**−**e**$[OTf]_2$ in reactions of **6b**−**e**[OTf] in neat MeOTf (Scheme 2c). Using a procedure previously applied to triphosphenium cations,[25] we have also realized that dialkylation occurs in mixtures of Me_4P_2 with 2 equiv of $GaCl_3$ and ^{t}BuCl to give **7i**$[GaCl_4]_2$, as illustrated in Scheme 2d.

Compounds **6a**−**e**[OTf], **7a**−**e**$[OTf]_2$, and **7i**$[GaCl_4]_2$ have been characterized in solution by $^{31}P\{^1H\}$ NMR spectroscopy (Table 1) and represent examples of isolated homonuclear spin pairs. For the symmetric cations in **7a**$[OTf]_2$, **7i**$[OTf]_2$, and **1**$[ClO_4]_2$,[14] the two phosphorus nuclei are magnetically equivalent and exhibit identical resonance frequencies independent of

(25) Burton, J. D.; Deng, R. M. K.; Dillon, K. B.; Monks, P. K.; Olivey, R. J. *Heteroat. Chem.* **2005**, *16*, 447−452.

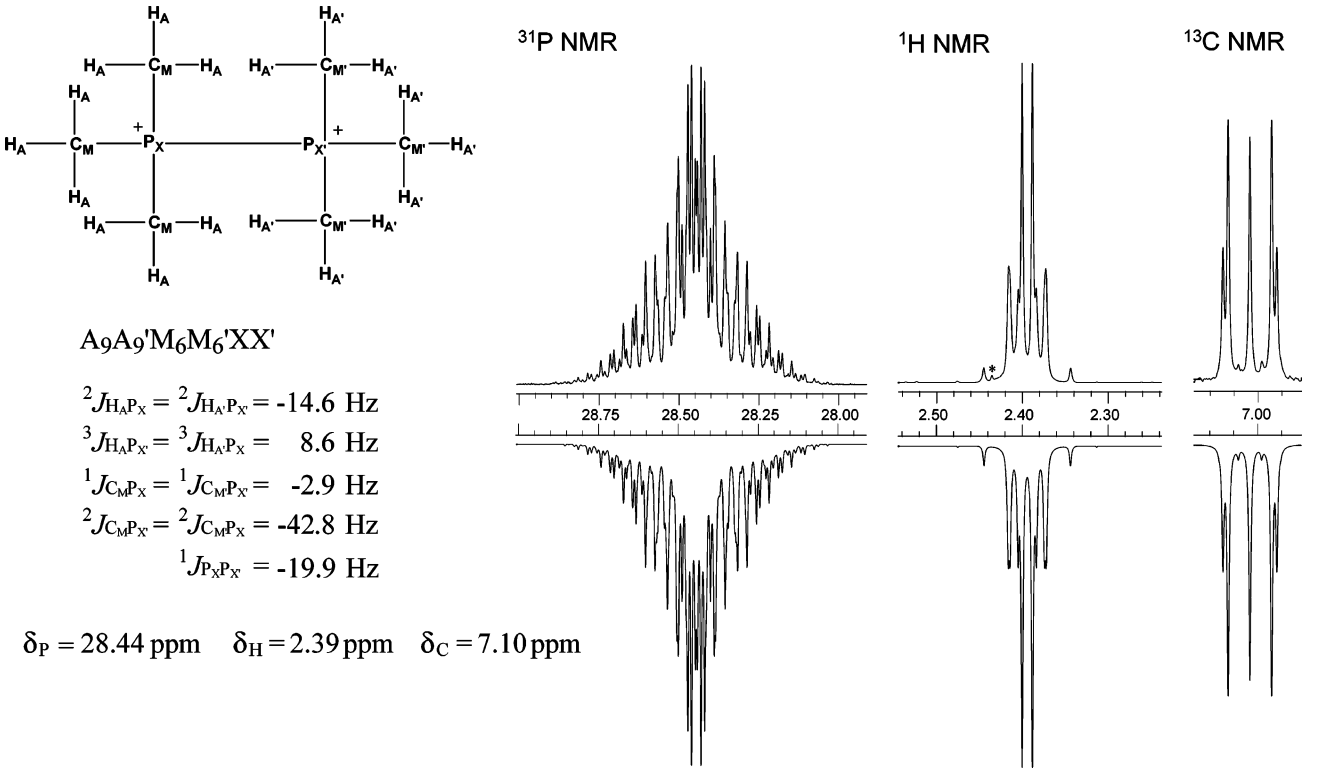

Figure 1. Experimental (upper) and simulated (lower) ^{31}P, ^{1}H, and ^{13}C NMR spectra of **7a**$[OTf]_2$ (in $[^2H]_3$-MeCN, RT); the asterisk indicates small amounts of impurities.

Table 1. ^{31}P NMR Data (202.46 MHz, $[^2H]_3$-MeCN, 300 K) for **1**$[ClO_4]_2$, **6a**−**e**[OTf], **7a**−**e**$[OTf]_2$, and **7i**$[GaCl_4]_2$

	$^{31}P\{^1H\}$ spin system[a]	$\delta(P_A)$ (ppm)	δ ($P_{B\ or\ X}$) (ppm)	$^1J_{PP}$[d] (Hz)
1$[ClO_4]_2$	A_2[c]	40	40	-
6a[OTf]	AX	17.60	−59.35	−274.3
6b[OTf]	AX	32.28	−63.08	−294.3
6c[OTf]	AX	24.20	−60.22	−296.0
6d[OTf]	AX	36.38	−54.77	−331.9
6e[OTf]	AX	42.26	10.81	−382.6
7a$[OTf]_2$	A_2[b]	28.44	28.44	−19.9
7b$[OTf]_2$	AX	37.12	28.22	−48.9
7c$[OTf]_2$	AB	29.39	28.08	−48.8[e]
7d$[OTf]_2$	AX	46.91	28.86	−74.4
7e$[OTf]_2$	AX	54.58	32.23	−93.6
7i$[GaCl_4]_2$	A_2[b]	45.75	45.75	−94.2[e]

[a] A $\Delta\nu/J \geq 10$ (AX), $< 10 > 0$ (AB), $\rightarrow 0$ (A_2). [b] Derived from simulation of the experimental spectra. [c] Coupling constant not reported in ref 14. [d] The absolute sign of the $^1J(PP)_{iso}$ in derivatives of **7** have been tentatively assigned to be negative. [e] The ^1H NMR spectra of **7c** and **7i** could not be simulated, and $^1J(P_AP_B)$ was obtained from the simulation of the ^{13}C NMR spectra.

the orientation of the spin pair in B_0, thus resulting in the observation of an A_2 spin system. For the nonsymmetric cations in **6a**−**e**[OTf] and **7b**, **d**, **e**$[OTf]_2$, the difference in resonance frequencies of the magnetically and chemically nonequivalent phosphorus centers is greater than the magnitude of the $^1J(P_AP_X)$, and an AX spin system is observed accordingly, while an AB spin system is observed for **7c**$[OTf]_2$. The NMR data obtained from simulated fitting of experimental spectra for the derivatives of **6** and **7** are presented in Table 1, together with the reported value for **1**$[ClO_4]_2$.[14] Additionally, these values were verified for derivatives of **7**$[OTf]_2$ by the simulation of the ^1H or ^{13}C NMR spectra.

For A_2 spin systems, analytical solutions[22] permit routine analysis. For example, Figure 1 shows the ^{31}P, ^1H, and $^{13}C\{^1H\}$ NMR spectra for **7a**$[OTf]_2$ as well as the band shape analysis[22] that defines an $A_9A_9'M_6M_6'XX'$ spin system, giving values for $^1J(P_XP_{X'})$ and $\delta(P_XP_{X'})$ and supporting the assignment of the $^{31}P\{^1H\}$ NMR signal for **7a**$[PF_6]_2$ at 27.9 ppm.[20] The known dependence of $^1J(PP)_{iso}$ on parameters such as oxidation state, coordination number, substituent electronegativity, stereochemistry, and the presence, or absence, of localized electron lone pairs may be used to predict the values of $^1J(PP)_{iso}$, but often the sign of $^1J(PP)_{iso}$ is unknown. In agreement with previous suggestions,[26−29] the absolute signs of the $^1J(PP)_{iso}$ values for derivatives of **6** and **7** have been tentatively assigned to be negative. The complexity of the ^1H NMR spectrum of **7i**$[GaCl_4]_2$ precluded simulation.

The δ_P values for P_A listed in Table 1 are greater when P_B bears larger alkyl groups (more methyl groups in the γ position relative to P_B) implicating a greater shielding due to the "γ effect".[30] Nevertheless, all values of δ_P are typical for phosphonium centers [range 28.4 to 54.6 ppm; Table 1]. The values of $^1J(PP)$ for derivatives of **7** [range −19.9 to −94.2 Hz; Table 1] are significantly smaller than those of the phosphinophosphonium cations **6** [range −284 to −382 Hz; Table 1]. The values of $^1J(PC)$, $^2J(PC)$, $^2J(PH)$, and $^3J(PH)$ are sensitive to conformational relationships.

(26) McFarlane, H. C. E.; McFarlane, W.; Nash, J. A. *Dalton Trans.* **1980**, 240−244.
(27) Aime, S.; Harris, R. K.; McVicker, E. M.; Fild, M. *Dalton Trans.* **1976**, 2144−2153.
(28) Forgeron, M. A. M.; Gee, M.; Wasylishen, R. E. *J. Phys. Chem.* **2004**, *108*, 4895−4908.
(29) Del Bene, J. E.; Elguero, J.; Alkorta, I. *J. Phys. Chem.* **2004**, *108*, 3662−3667.
(30) Harris, R. K.; Norval, E. M.; Fild, M. *J. Chem. Soc., Dalton Trans.* **1979**, 826−831.

Table 2. Crystal and Refinement Data for **7a**$[OTf]_2$, **7b**$[OTf]_2$, **7d**$[OTf]_2$, and **7i**$[GaCl_4]_2$

	7a$[OTf]_2$	**7b**$[OTf]_2$	**7d**$[OTf]_2$	**7i**$[GaCl_4]_2$
formula	$C_8H_{18}F_6O_6P_2S_2$	$C_{11}H_{24}F_6O_6P_2S_2$	$C_{14}H_{30}F_6O_6P_2S_2$	$C_{12}H_{30}P_2Ga_2Cl_8$
molecular weight [g mol^{-1}]	450.28	492.36	534.44	659.34
color, habit	colorless, plate	colorless, plate	colorless, irregular	colorless, irregular
crystal system	rhombohedral	monoclinic	triclinic	orthorhombic
space group	$R\bar{3}m$	$P2/c$	$P\bar{1}$	$Pna2(1)$
a [Å]	9.228(3)	15.765(6)	8.750(3)	17.749(2)
b [Å]	9.228(3)	11.994(5)	11.566(4)	10.204(1)
C [Å]	17.826(5)	24.584(8)	12.245(5)	14.494(2)
α [deg]	90.0	90.0	88.744(6)	90.0
β [deg]	90.0	114.619(5)	74.948(4)	90.0
γ [deg]	120.0	90.0	76.431(4)	90.0
V [Å^3]	1314.6(7)	4226(3)	1162.3(7)	2625.0(6)
Z	3	8	2	4
T [K]	213(2)	173(1)	198(1)	198(1)
crystal size [mm^3]	0.35 × 0.20 × 0.05	0.50 × 0.35 × 0.10	0.40 × 0.30 × 0.20	0.20 × 0.20 × 0.15
ρ_c [mg m^{-3}]	1.706	1.548	1.527	1.668
F(000)	690	2032	556	1320
$\lambda_{MoK\alpha}$, Å	0.71073	0.71073	0.71073	0.71073
θ_{min} [deg]	2.79	1.42	1.72	2.29
θ_{max} [deg]	27.43	27.50	27.50	27.49
index range	$-11 \le h \le 11$ $-10 \le k \le 11$ $-22 \le l \le 23$	$-20 \le h \le 20$ $-14 \le k \le 15$ $-31 \le l \le 31$	$-11 \le h \le 11$ $-13 \le k \le 14$ $-15 \le l \le 14$	$-22 \le h \le 23$ $-12 \le k \le 11$ $-17 \le l \le 18$
μ [mm^{-1}]	0.569	0.479	0.442	2.987
absorption correction	SADABS	SADABS	SADABS	SADABS
reflections collected	3007	28 485	7997	17 073
reflections unique	399	9473	5008	5590
R_{int}	0.0415	0.0439	0.0170	0.0438
reflection obsd [$F > 2\sigma(F)$]	366	6904	4169	4174
residual density [e Å^{-3}]	0.503, −0.918	0.652, −0.503	0.996, −0.627	0.830, −0.424
parameters	29	546	391	227
GOF	1.377	1.047	1.059	0.990
R_1 [$I > 2\sigma(I)$]	0.0391	0.0400	0.0479	0.0376
wR_2 (all data)	0.1061	0.1177	0.1413	0.0819

Compounds **7a**$[OTf]_2$, **7b**$[OTf]_2$, **7d**$[OTf]_2$, and **7i**$[GaCl_4]_2$ have been crystallographically characterized confirming their identities as the first examples of salts containing hexaalkylated diphosphonium dications including a symmetrically substituted derivative (**7a**), nonsymmetrically substituted homoleptic derivatives (**7b** and **7d**), and a symmetrically substituted heteroleptic (**7i**) derivative. Crystal data for **7a**$[OTf]_2$, **7b**$[OTf]_2$, **7d**$[OTf]_2$, and **7i**$[GaCl_4]_2$ are presented in Table 2. Table 3 lists selected structural parameters for the dications, and Figure 2 shows an ORTEP view for each dication.

In the solid state, the P−P bonds and S−C bonds of **7a**$[OTf]_2$ lie on the same threefold axis with an ideal staggered conformation [C^{ii}−P−P^{iii}−C 60.0(2)°], as illustrated in Figure 3. The $-SO_3$ group of the triflate anion is proximal to the dication, and the $-CF_3$ groups are neighbors between formula units. The cations and anions are hexagonally close packed involving H···F contacts [C−H···F 3.192(3) Å; 123.4(19) °].[31,32] In contrast to the crystallographically ideal gauche conformation observed for **7a**$[OTf]_2$, **7b**$[OTf]_2$ and **7d**$[OTf]_2$ do not adopt crystallographic threefold symmetry. Compound **7b**$[OTf]_2$ crystallizes in the monoclinic space group $P2/c$ with eight formula units in the unit cell. Although one of the PEt_3 groups of the two crystallographically independent molecules in **7b**$[OTf]_2$ is disordered, the interatomic distances and bond angles are almost identical in the two independent molecules. The main structural features of the core of **7b**$[OTf]_2$ resemble those of **7a**$[OTf]_2$. In **7d**$[OTf]_2$, the *iso*-propyl group at C3 adopts a *transoid* H−C3−P1−P2 conformation, while the *iso*-propyl groups at C1 and C2 are twisted, leading to a gauche H−C−P1−P2 conformation. The C−P1−C angles involving the C atom of the *transoid* H−C3−P1−P2 moiety are significantly smaller [107.7 (1), 110.4(1)°] than that of the other *iso*-propyl groups (C1−P1−C2 114.7(1)°). This may be explained by the increase of apparent "1,3-dimethyl strain", exhibited by short contacts C7···C9 3.376(8), C8···C10 3.518 Å [sum of the van der Waals radii r_w(C) = 3.40 Å][33] between the two twisted *iso*-propyl groups in **7d**$[OTf]_2$. These interactions are illustrated by the arrows in Figure 2. The C1−P1−P2−C4 gauche dihedral angle (ω) in **7a**$[OTf]_2$ is crystallographically imposed ($\omega = 60°$), in contrast to **7d**$[OTf]_2$ [$\omega = 40.8(2)°$], which is influenced by the "1,3-dimethyl strain" interaction of PMe_3 with P^iPr_3, thus rendering the conformation of **7d** as an intermediate between the staggered and eclipsed conformations. The steric demand of the *iso*-propyl groups in **7b**$[OTf]_2$ and **7d**$[OTf]_2$ and the *tert*-butyl groups in **7i**$[GaCl_4]_2$ is accommodated by relatively long P−C bonds at the more sterically loaded P1 site in **7b**$[OTf]_2$ and **7d**$[OTf]_2$ [range 1.807(2) to 1.831(3)Å] and for the *tert*-butyl P−C bonds in **7i**$[GaCl_4]_2$ [1.838(5); 1.828(5)Å]. Correspondingly, the P−CH_3 bonds in **7a**$[OTf]_2$ [1.783(3) Å], **7b**$[OTf]_2$ and **7d**$[OTf]_2$ [range at P2 1.780(2) to 1.790(3) Å], and **7i**$[GaCl_4]_2$ [range 1.779(5) to 1.799(5) Å] are consistently shorter.

(31) Bondi, A. *J. Phys. Chem.* **1964**, *68*, 441−451.
(32) Spek, A. L. *J. Appl. Crystallogr.* **2003**, *36*, 7−13.
(33) Neumann, F.; Teramae, H.; Dowing, J. H.; Michl, J. *J. Am. Chem. Soc.* **1998**, *120*, 582.

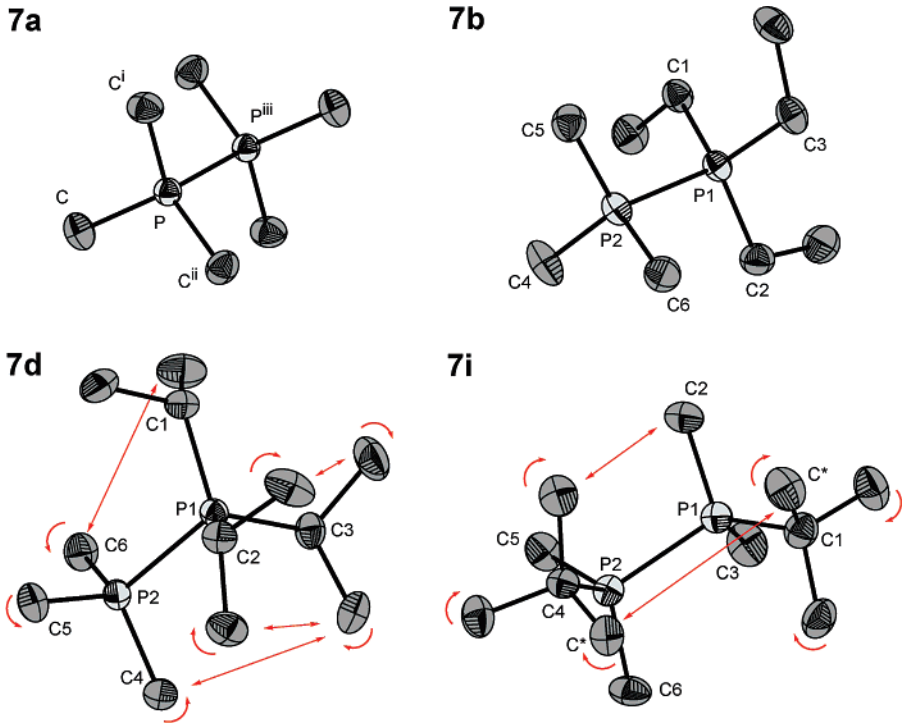

Figure 2. ORTEP view of the molecular structure of the dication in **7a**$[OTf]_2$, **7b**$[OTf]_2$, **7d**$[OTf]_2$, and **7i**$[GaCl_4]_2$ in the solid state. For **7i** only the g+ enantiomer is shown. Arrows indicate "1,3- and 1,4 dimethyl strain" and the rotation which minimizes these interactions. Amplitude displacement ellipsoids are depicted at 50% probability (hydrogen atoms are omitted). [Symmetry codes for **7a**: (i) $-x + y$, $1 - x$, z; (ii) $1 - y$, $1 + x - y$, z, (iii) $^2/_3 + x - y$, $^4/_3 - y$, $^1/_3 - z$.]

Table 3. Selected Interatomic Distances and Bond Angles for **7a**$[OTf]_2$, **7b**$[OTf]_2$, **7d**$[OTf]_2$, and **7i**$[GaCl_4]_2$

	7a$[OTf]_2$	**7b**$[OTf]_2$	**7d**$[OTf]_2$	**7i**$[GaCl_4]_2$
		[Å]		
P1−P2[a]	2.198(2)[b]	2.216(1)	2.2370(9)	2.232(2)
P1−C1	1.783(3)[b]	1.807(2)	1.830(3)	1.838(5)
P1−C2		1.810(2)	1.831(2)	1.779(5)
P1−C3		1.811(2)	1.829(3)	1.799(5)
P2−C4		1.780(2)	1.790(3)	1.828(5)
P2−C5		1.786(2)	1.789(3)	1.796(4)
P2−C6		1.787(2)	1.787(3)	1.791(5)
		[deg]		
P2−P1−C1	107.06(9)[b]	104.1(8)	107.50(9)	118.8(2)
P2−P1−C2		110.1(8)	107.23(9)	106.1(2)
P2−P1−C3		107.5(8)	109.20(9)	103.4(2)
P1−P2−C4		107.42(9)	109.7(1)	116.2(2)
P1−P2−C5		109.69(9)	108.4(1)	108.6(2)
P1−P2−C6		106.68(9)	110.1(1)	101.2(2)
C1−P1−C2	111.77(8)[b]	112.3(1)	114.7(1)	112.2(2)
C2−P1−C3		110.3(1)	107.7(1)	107.0(2)
C3−P1−C1		112.2(1)	110.4(1)	108.6(2)
C4−P2−C5		110.7(1)	111.5(2)	110.7(2)
C5−P2−C6		110.5(1)	110.0(1)	107.0(2)
C6−P2−C4		111.8(1)	112.3(2)	116.2(2)
		[deg]		
C1−P1−P2−C4[a]	60.0(2)[b]	58.3(1)	40.8(2)	56.5(3)
C1−P1−P2−C5		178.6(1)	162.7(1)	176.4(3)
C1−P1−P2−C6		−61.7(1)	−77.0(1)	−71.2(3)

[a] For comparison: P−P in $[(Et_2N)_3P-P(NEt_2)_3][ClO_4]_2$ (**1**$[ClO_4]_2$) = 2.364(3) Å and N−P−P−N torsion angle $\omega = 30°$.[14] [b] In Figure 2, the $P-P^{iii}$, P−C, $C-P-P^{iii}$, $C-P-C^{i}$, $C^{ii}-P-P^{iii}-C$ numbering scheme differs from those provided in the CIF files, to allow for a direct comparison within the text. [Symmetry codes: (i) $-x + y$, $1 - x$, z; (ii) $1 - y$, $1 + x - y$, z; (iii) $^2/_3 + x - y$, $^4/_3 - y$, $^1/_3 - z$.]

NBO analysis[34] calculations based on the structural parameters observed in the solid state indicate "secondary hyperconjugation"[35] effects within the bulky substituents. The interaction of occupied σ_{CH} orbitals of the methyl groups in both the *iso*-propyl (**7d**) and the *tert*-butyl groups (**7i**), with the corresponding empty σ^*_{PC} antibonding orbitals, leads to a transfer of electron density from bonding to antibonding orbitals as reflected by P−C bonds which are elongated with respect to typical values. Computational methods generally assume that saturated chains of the type A_4X_{10} (A = C or Si; X = H, F, Cl, Br, Me, or SiH_3) only adopt six distinct stable conformers with respect to rotation around a skeletal A−A bond [AAAA dihedral angles of ω 60° (gauche), 180° (trans), and ω 90° (ortho)].[33] Recently, electron diffraction studies of Si_4Me_{10}[36] have shown the presence of the *anti* and *gauche* conformer in the gas phase. Cation **7i** can be considered a solid state example of A_4X_{10} ($P_2C_2Me_{10}$), existing as a racemic crystalline material with two enantiomeric gauche forms (g+, g−) exhibiting C1−P1−P2−C4 dihedral angles of $\omega = 56.5(3)°$ (right-handed helix, g+) and $\omega = -56.5(3)°$ (left-handed helix, g−). The "1,3- and 1,4-dimethyl strain" in **7i** leads to a C*···C* separation of 3.933(7) Å, as indicated in Figure 2, primarily through clockwise rotation of the two *tert*-butyl groups. This interaction explains the decrease of the dihedral angle from $\omega = 60.0°$ (ideal staggered) to 56.5(3)° (Table 3).

The P−P bond lengths in the cyclic compounds **2**,[15] **3**,[16] and **4**[17] [range 2.165(2)−2.2498(9) Å] are shorter than that in **1**[14] [2.364(3) Å] perhaps due to the restrictions imposed by the cyclic structures. However, P−P bonds in **7a**, **7b**, **7d**, and **7i** [range 2.198(2) to 2.2370(9) Å] are very similar to those observed in neutral, anionic and cationic cyclic, and acyclic *catena*-phosphorus compounds [2.17 to 2.24 Å]. Preliminary

(34) Reed, E. D.; Carpenter, J. E., and Weinhold, F. *NBO*, version 3.1; 2006.

(35) Reed, D. E.; Weinhold, F. *Isr. J. Chem.* **1991**, *31*, 277−285.

(36) Belakov, A. V.; Haaland, A.; Shorokhov, D. J.; West, R. *J. Organomet. Chem.* **2000**, *597*, 87−91.

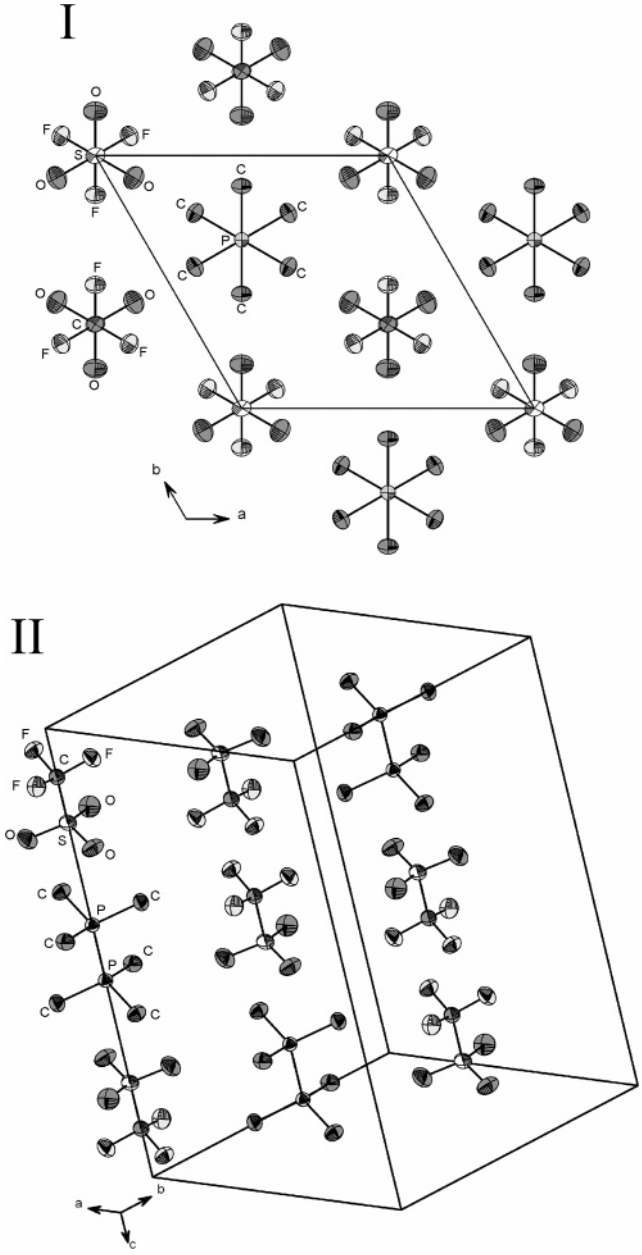

Figure 3. (I) Unit cell of the solid-state structure of **7a**$[OTf]_2$ viewed down the *c*-axis. (II) Perspective view of the cation/anion arrangement parallel to the *c*-axis.

MO and NBO calculations on **7a** support the existence of a typical, localized single bond between the two phosphonium centers and are in agreement with the calculated NLMO bond order 0.9527, the Wiberg bond indices (WBI), and the calculated partial charges (Figure 4). The calculated natural atomic orbital population (NAO) net charges are $q(P) = +1.270$, $q(C) = -1.080$, and $q(H) = +0.330$ indicating that the positive charge is principally located on the phosphorus atoms. This further suggests that the P−P bond length is independent of both the coordination number and the valence state of the phosphorus atoms. The P−P bond length does, however, correlate with the change in the observed dihedral angle [$\omega = 30°$ (**1**) < 40.8(2)° (**7d**) < 56.5(3)° (**7i**) < 58.3(1)° (**7b**) < 60.0(2)° (**7a**), Table 3].

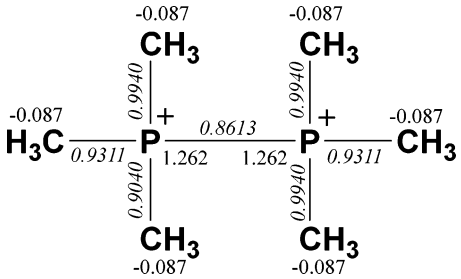

Figure 4. NBO analysis of **7a**$[OTf]_2$ along with the WBI (italic) and NPA charges (roman) with hydrogen atoms summed into heavy atoms.

Summary

Dialkylation of P−P diphosphines, as well as methylation of P−P phosphinophosphonium cations, provide versatile synthetic approaches to fundamentally important prototypical examples of hexaalkylated diphosphonium dications that define the origin of a potentially extensive and diverse *catena*-phosphorus chemistry, paralleling *catena*-carbon chemistry. The quantitative nature of the reactions bodes well for the development of polyphosphonium chemistry.

Acknowledgment. We thank the Natural Sciences and Engineering Research Council of Canada, the Killam Foundation, the Canada Research Chairs Program and the Alexander von Humboldt-Stiftung (Humboldt-Fellowship for J.J.W., Lynen program) for funding.

Supporting Information Available: X-ray crystallographic files in CIF format of **7a**$[OTf]_2$, **7b**$[OTf]_2$, **7d**$[OTf]_2$, and **7i**$[GaCl_4]_2$ as well as selected NMR spectra and computational details. This material is free of charge via the Internet at http://pubs.acs.org.

JA071306+